Determination of Diesel Sprays Characteristics in Real Engine In-Cylinder air Density and Pressure Conditions

Raul Payri*, F. J. Salvador, J. Gimeno, V. Soare
CMT-Motores Térmicos, Universidad Politécnica de Valencia, Camino de Vera s/n, E-46022 Spain

The present paper centers on the establishment of a quantified relationship between the macroscopic visual parameters of a Diesel spray and its most influential factors. The factors considered are the ambient gas density, as an external condition relative to the injection system, and nozzle hole diameter and injection pressure as internal ones. The main purpose of this work is to validate and extend the different correlations available in the literature to the present state of the Diesel engine, i.e. high injection pressure, small nozzle holes, severe cavitating conditions, etc. Five mono-orifice, axi-symmetrical nozzles with different diameters have been studied in two different test rigs from which one can reproduce solely the real engine in-cylinder air density, and the other, both the density and the pressure. A parametric study was carried out and it enabled the spray tip penetration to be expressed as a function of nozzle hole diameter, injection pressure and environment gas density. The temporal synchronization of the penetration and injection rate data revealed a possible explanation for the discontinuity observed as well by other authors in the spray's penetration law. The experimental results obtained from both test rigs have shown good agreement with the theoretical analysis. There have been observed small but consistent differences between the two test rigs regarding the spray penetration and cone angle, and thus an analysis of the possible causes for these differences has also been included.

Key Words : Spray, Penetration, Correlations, Diesel Injection, Nozzle Geometry

Nomenclature

a-e : Coefficients used in correlations
k : Constant used in correlations
k-factor : Convergence or divergence factor of the nozzle orifice. $k\text{-}factor = 0.1 \cdot (\phi_i - \phi_o)$
K : Cavitation number
L : Length of the nozzle's orifices
$\dot{m}_f$: Mass flux.
$\dot{M}_o$: Momentum flux
P_{back} : Backpressure
P_{in} : Injection pressure
r : Orifice inlet rounding
U_o : Orifice outlet velocity
t : Time
t_t : Transition time.
S : Spray tip penetration

Greek Symvols

ϕ_i : Inlet diameter of the nozzle's orifices
ϕ_o : Outlet diameter of the nozzle's orifices
ΔP : Pressure drop, $\Delta P = P_{in} - P_{back}$
ρ_a : Ambient density
ρ_f : Fuel density
θ : Spray cone angle

Subscripts

crit : Critical cavitation conditions

* Corresponding Author,
E-mail : rpayri@mot.upv.es
TEL : +34-963879658; **FAX** : +34-963877659
CMT-Motores Térmicos, Universidad Politécnica de Valencia, Camino de Vera s/n, E-46022 Spain. (Manuscript **Received** February 22, 2005; **Revised** September 29, 2005)

1. Introduction

The aim of the fuel injection process in Diesel engines is the preparation of the fuel-air mixture

in order to achieve efficient combustion process with low pollutants formation. This process is strongly influenced by the spray behavior which depends on several parameters. These parameters can be classified into two groups : parameters related to the Diesel injection system and parameters related to the environment where the spray is injected.

In this paper, the sprays from five axi-symmetrical nozzles with different diameters are characterized in two different test rigs. Both of them can reproduce a range of gas densities that can be encountered inside the combustion chamber in the moment the injection starts. However, due to the fact that they achieve this in different ways, they provided a good opportunity to check the validity of the theoretical assumption that the gas density is the only factor influencing the spray behavior in non-evaporative conditions.

A wide parametric study was performed and has permitted to quantify the effects of the injection pressure, nozzle orifice diameter and ambient gas density on the spray tip penetration. The results obtained from both experimental facilities have been compared between themselves and with the results achieved through a theoretical analysis.

The paper is structured in five main sections. First, a short review of the most significant works available in the literature about Diesel sprays is presented. In this part, a simple dimensional analysis is made which led to a penetration expression as a function of several parameters. The experimental facilities are described in the second section in which the sulphur hexafluoride test rig and nitrogen test rig are briefly described. The more important characteristics of the image acquisition system and the image processing software are also presented. In the third section the experimental procedure, the nozzles used and the experimental conditions are shown. Next, in section four the results obtained are presented, and lastly, in section five an analysis based on the spray macroscopic parameters is carried out.

2. Background

Several experimental and theoretical works have been performed on free gaseous and Diesel sprays. Most of them conclude with empirical or semi-empirical laws to predict the penetration and the spray cone angle as a function of several parameters. The experimental results of these works are quite diverse (and sometimes contradictory) depending on the experiments themselves as well as the authors. In this way the work of Hay and Jones (1972) includes a critical revision on the correlations available in the literature proposed for Diesel sprays and concludes that the best ones are those proposed by Dent (1971) and Wakuri et al.(1960). Dent's correlation is based on the theory of the gaseous injection, whilst Wakuri proposes a penetration law which depends on the spray cone angle. Later, Hiroyasu and Arai (1990) proposed a different penetration law divided in two regions : before and after the break-up time.

All these experimental correlations involve the same parameters (ΔP, ϕ_o, ρ_a, t) with more or less the same weights. Therefore, it seems clear that for a given nozzle hole, the most influential parameters for the spray penetration are the gas density, the injection pressure and the time elapsed from the start of injection.

Such expressions can be obtained by performing a dimensional analysis with the following variables :

- Ambient gas density (ρ_a).
- Time (t) from the start of injection.
- Instantaneous momentum flux ($\dot{M}_o$) through the orifice. This parameter brings together the injection pressure and the nozzle diameter effects (Desantes et al., 2003 ; Payri et al., 2005).

For a simple rectangular injection rate, $\dot{M}_o$ is given by :

$$\dot{M}_o = \dot{m}_f \cdot U_o = \rho_f \cdot \frac{\pi}{4} \cdot \phi_o^2 \cdot U_o^2 \qquad (1)$$

Where $\dot{m}_f$ is the instantaneous mass flow rate and U_o is the outlet velocity.

Applying the π Vashy-Buckingham theorem :

$$S(t) \propto \rho_a^{-1/4} \cdot M_o^{1/4} \cdot t^{1/2} \qquad (2)$$

Introducing the expression of $\dot{M}_o$ given by (1), applying the Bernoulli's equation through the

nozzle hole, the spray tip penetration is given by:

$$S(t) \propto \rho_a^{-1/4} \cdot \Delta P^{1/1} \cdot \phi_o^{1/2} \cdot t^{1/2} \quad (3)$$

Hence the dependencies found are those proposed by Hiroyasu et al.(1990), Wakuri et al.(1960) and Dent (1971) (in this last case without the fuel evaporation term).

3. Experimental Facilities

The macroscopic spray characterization has been performed in two different injection test rigs that both reproduce the high gas density encountered in a Diesel engine combustion chamber, with the difference that one of them reproduces also pressure conditions existing in the real engine when the injection starts. However, it should be pointed out that isothermal conditions are considered and no evaporation is present. These rigs, as well as the image-acquisition system and image processing software employed for the investigation, will be briefly described in the next paragraphs.

3.1 Sulphur hexafluoride (SF_6) test rig

This testing facility consists of a constant-volume vessel where the spray is produced and visualised, and a set of pipes connected to a Roots compressor that ensures a continuous scavenging of the gas inside the vessel. The gas flow velocity is comparatively low at approximately 0.7 m/s, and thus it is not expected to influence the spray's behaviour.

The gas filling the test rig is sulphur hexafluoride (SF_6), which is inert, avoiding combustion. Due to its high molecular mass it can reach the density values that normally occur in a Diesel engine at the moment of injection (20 to 50 Kg/m^3) at much lower pressures (0.2 to 0.7 MPa). More details of the SF6 test rig are available in Arrègle et al.(1999).

3.2 Nitrogen (N_2) test rig

The nitrogen test rig is similar in concept to the SF_6 rig, but it reproduces both the high gas pressure and density encountered in the Diesel engine. The rig has been designed for a maximum pressure of 6 MPa. The continuous flow of the nitrogen is ensured by piston compressors that feed it into a constant-pressure tank, from where it passes through an electronically-controlled valve and into the injection rig. The temperature of the nitrogen is controlled and can be set to values between 15 and 50℃ in order to obtain the desired density inside the chamber. More details of the nitrogen test rig are available in F. Payri et al.(2004).

3.3 Image acquisition system and image processing software

In this study, the visualization of the sprays is carried out by the shadowgraphy technique (Pastor et al., 2001). The images are taken with a 12-bit colour camera with a spatial resolution of 1280×1024 pixels, a minimum exposure time of 50 microseconds and with a jitter of (5 microseconds. Illumination is created with two electronic flashes, with duration of 10 microseconds and synchronized with the camera in such a way that the maximum intensity occurs in the middle of the camera exposure time.

The injection and its synchronization with the camera and the flash are managed by a purpose-built system featuring an ECU, allowing for very low injection frequency (0.25 Hz). This long time interval between injections is required in both test rigs in order to remove the fuel droplets from the previous injection, and thus maintain good optical access to the spray. Figure 1 shows a sample

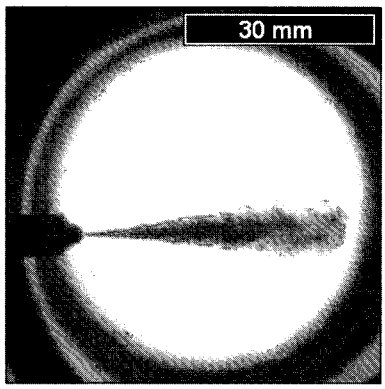

Fig. 1 Sample of an image (scaled) of a spray from one of the axi-symmetrical nozzles tested

Table 1 Dimensional characteristics of the nozzles

Nozzle	ϕ_i [μm]	ϕ_o [μm]	*k-factor* [−]	R [μm]	r/ϕ_o [−]	L/ϕ_o [−]
1	119	119	0.0	8	0.067	8.4
2	139	140	−0.1	12	0.086	7.1
3	163	165	−0.2	8	0.048	6.1
4	177	183	−0.6	12	0.066	5.5
5	204	206	−0.2	6	0.029	4.9

spray image resulting with this technique.

The images were taken at steps of 25 microseconds throughout the injection period. A minimum of 5 images per step were used for the analysis presented here. An injector energizing time was 1.5 ms. This way, a typical characterization of an operating point consists of 425 pictures.

Details of the image acquisition system and processing software are available in Pastor et al. (2001).

3.4 Injection system

The same injection system was used to generate Diesel sprays in both test rigs. It consists of commercially available components: a high pressure volumetric pump (driven by a motor), a common rail ready to receive up to four injectors, and one induction-coil injector. Appropriated software to govern the electronic system is used.

There have been used 5 cylindrical mono-orifice nozzles with diameters ranging from 119 μm to 206 μm especially manufactured for this research. The nozzle outlet diameters and dimensional characteristics were obtained using the silicone technique (Macian et al., 2003b) and the exact dimensions can be found in Table 1.

4. Experimental Conditions

Table 2 summarizes the values of the different test parameters considered in this work for spray visualization.

As it can be seen from Table 2, the actual pressure differential is higher in the SF_6 rig although the injection pressures used were the same for both test rigs. This is because it requires less pressure to obtain the same densities as in the N_2 test rig. It can also be noticed that only the four lowest densities were tested in the SF_6 rig because of its limitation through construction to a maximum pressure of 0.7 MPa.

In order to work out the density as a function of the pressure and temperature inside the chamber, perfect gas equation of state was considered for nitrogen, while for SF_6 the Van der Waals equation for real gases was required. In this case, the values obtained are in agreement with the characterization of the SF_6 made by Hurly et al.

Table 2 Experimental conditions

	ϕ_o [μm]	P_{in} [MPa]	P_{back} [MPa]	ρ_a [kg/m^3]
N_2	**119**	50/80/130	1/2/3/4/5/6	12/24/35/46/58/69
	140	50/80/130	1/2/3/4/5/6	12/24/35/46/58/69
	165	50/80/130	1/2/3/4/5/6	12/24/35/46/58/69
	183	50/80/130	1/2/3/4/5/6	12/24/35/46/58/69
	206	50/80/130	1/2/3/4/5/6	12/24/35/46/58/69
SF^6	**119**	50/80/130	0.087/0.28/0.47/0.67	11/23/35/48
	140	50/80/130	0.087/0.28/0.47/0.67	11/23/35/48
	165	50/80/130	0.087/0.28/0.47/0.67	11/23/35/48
	183	50/80/130	0.087/0.28/0.47/0.67	11/23/35/48
	206	50/80/130	0.087/0.28/0.47/0.67	11/23/35/48

Table 3 Physical properties of N_2 and SF_6

	N_2	SF_6	Conditions
Viscosity (kg/ms)	$1.77\ 10^{-5}$	$1.61\ 10^{-5}$	25℃, 1 atm
Density (kg/m^3)	1.15	6.14	25℃, 1 atm
Refractive index	1.000298	1.000783	25℃, 1 atm
Sound velocity (m/s)	347.46	136	25℃, 1 atm
Melting point (K)	63.05	222.2	1 atm
Boiling point (K)	77.36	209.1	1 atm
Molecular Weight (g/mol)	28.0134	146.05	—

(2000), where other properties such as molecular viscosity and speed of sound are also available. The temperature inside both rigs was kept constant at 25℃. Table 3 is a comparison of physical properties between N_2 and SF_6 at this temperature.

Considering the pressure drop, it is appropriate to note that cavitation phenomenon is likely to occur because of the high pressure difference, and furthermore, cylindrical nozzles (like those used in this investigation) are more prone to cavitate than other types of geometries as for example convergent nozzles (Payri et al., 2000; 2002; Macian et al., 2003a; Koo, 2003).

For cavitating nozzles, the critical cavitation number is defined as K_{crit}, corresponding to the pressure drop at which cavitation starts in the injector orifice. When this phenomenon occurs at a given level of the injection pressure it is revealed through the stabilization of the mass flow rate across the orifice, despite further decrease in discharge pressure (choking) (Desantes et al., 2003; Macian et al., 2003a; Payri et al., 2004; 2004a).

It is known that the spray cone angle increases immediately when cavitation occurs in the orifice, and its variation is directly proportional to the length of the in-orifice flow affected by this phenomenon (Macian et al., 2003; Payri et el., 2004). At the point where cavitating flow extends to the outlet, cavitation is assumed to be fully developed and thus the value of the angle is stabilized.

However, in the present case this transitional behavior was avoided because the pressure drops employed (P_{in}-P_{back}) were sufficient to ensure the fully developed cavitation even for the lowest pressure difference, i.e. injection pressure of 50 MPa in the nitrogen test rig. In fact, the critical cavitation number, K_{crit}, for the five axy-simmetrical nozzles are characterized in Desantes et al. (2005). This characterization confirmed the fully developed cavitation condition.

5. Results

The macroscopic parameters of the spray that were characterized are the penetration (S) and the spray cone angle (θ). The spray cone angle is calculated by taking into consideration only the first 60% of the total penetration length (Pastor et al., 2003).

In the Figures 2~6 the mean values of penetration and cone angle data are represented for the different nozzles, operating in the nitrogen test rig at an injection pressure P_i=130 MPa and different chamber densities.

The standard deviation found for penetration (not represented in the figures) was around 0.8 mm. and for the cone angle was 1.5°; therefore, the accuracy of the experimental results was very high. Figures 2~6 also reveal the considerable influence that gas density has over the spray tip penetration and spray cone angle. This will be studied in the next section.

5.1 Analysis of the spray images. Comparison between SF_6 and N_2 test rig results

One of the most important conclusion of the results was that differences were observed in spray tip penetration and spray cone angle between the

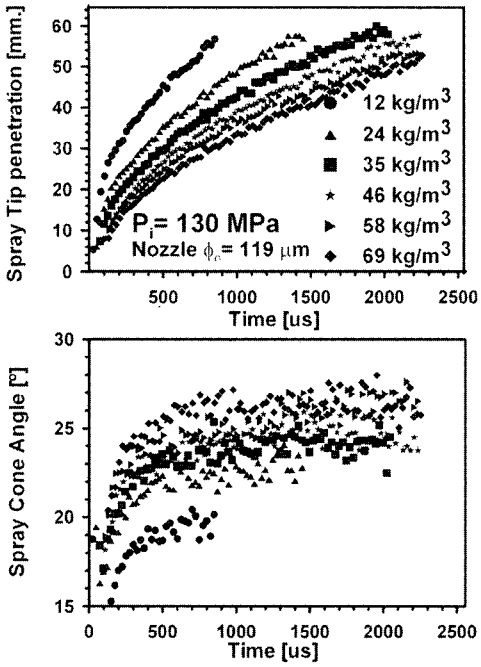

Fig. 2 Mean values of penetration and cone angle at different chamber density. (ϕ_o=119 μm and P_i=130 MPa)

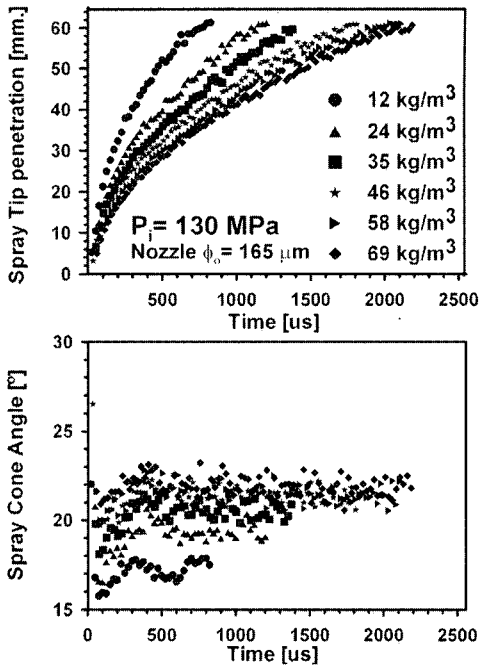

Fig. 4 Mean values of penetration and cone angle at different chamber density. (ϕ_o=165 μm and P_i=130 MPa)

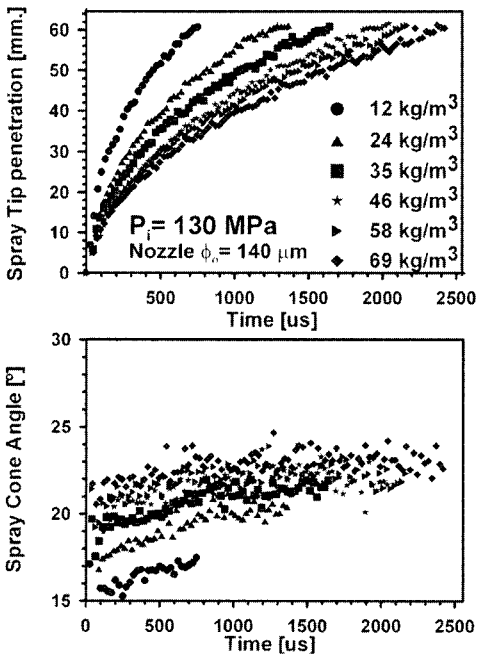

Fig. 3 Mean values of penetration and cone angle at different chamber density. (ϕ_o=140 μm and P_i=130 MPa)

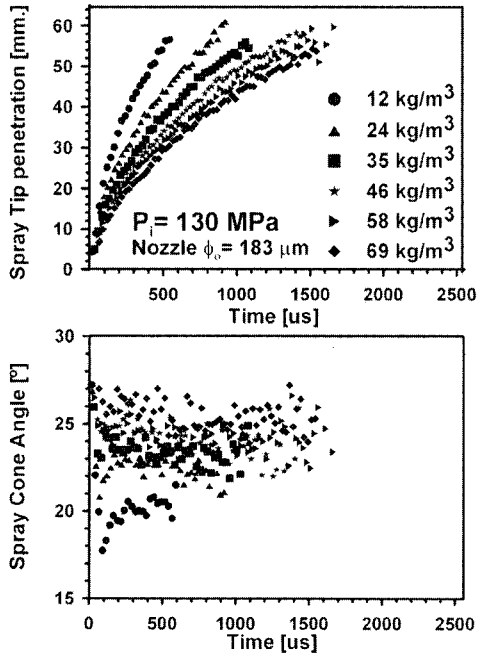

Fig. 5 Mean values of penetration and cone angle at different chamber density. (ϕ_o=183 μm and P_i=130 MPa)

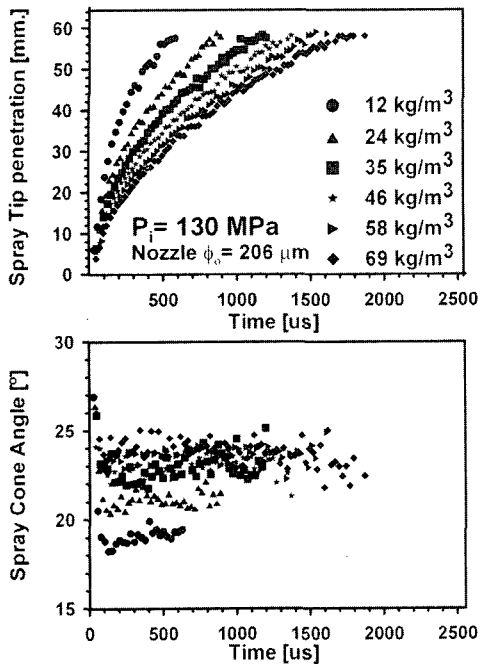

Fig. 6 Mean values of penetration and cone angle at different chamber density. (ϕ_o=206 μm and P_i=130 MPa)

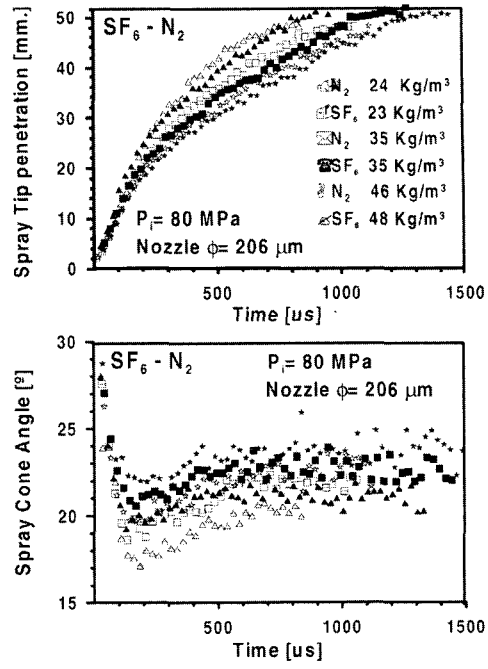

Fig. 7 Comparison of results from N_2 test rig and SF_6 test rig for the nozzle with ϕ_o=206 μm and P_i=80 MPa at different chamber density

two test rigs, although the chamber density was the same. This difference has been noted for all injection pressures and densities. For example, in Figure 7 are shown the results of spray tip penetration and spray cone angle from both rigs. These results correspond to the nozzle with ϕ= 206 μm, injection pressure of 80 MPa and different chamber densities.

As shown in Figure 7, differences are found especially in the developed region of the spray. It can be observed that penetration in the SF_6 case is on average around 6% higher than in N_2 case. These differences are more important if we compare the spray cone angle. In this case, the angle measured in the sulphur hexafluoride test rig can be about 10% smaller than in the nitrogen test rig. Higher penetration corresponding to a lower spreading angle for the SF_6 test rig is consistent with the conservation of momentum.

One possible explanation for these differences could be the distinct ΔP. For example, in the case of 35 Kg/m^3 (with P_i=80 MPa), ΔP_{N2}=77 MPa and ΔP_{SF6}=79.5 MPa. Nevertheless, if we take into account equation (3) (as will be seen later, this equation fits well with the experimental results), the influence of ΔP on the spray penetration is affected by the exponent 0.25. It means that the differences in penetration due to the different ΔP should be only around 0.8%.

There are also no differences neither in the ambient turbulence nor in the flow pattern between the SF_6 and N_2 test rig. In both test rigs the gas is continuously circulated, at a velocity of approximately 1 m/s, which is relatively low, so that it should not affect the diesel spray.

Another phenomenon that could affect the results is cavitation. As stated before, cavitation depends of the difference between the injection pressure and back pressure.

Due to the fact that the P_{back} in the SF_6 test rig is always lower than in the N_2 test rig, stronger cavitation is expected to occur inside nozzles in the SF6 test rig injection conditions (Desantes et al, 2003 ; Payri et al., 2005 ; Macian et al., 2003a ; Payri et al., 2004a). However, it is known that cavitation produces a considerable increase in the

spray cone angle. This does not match with the results obtained in which the spray cone angle in SF_6 is smaller than in N_2. Finally, one possible cause for the differences found could be the generation of shock waves in SF_6 and their absence in N_2 as noticed by Cheong et al.(2004). In fact, the speed of sound in N_2 at a room temperature of 25℃ is about 347 m/s while in SF_6 is 136 m/s (Hurly et al., 2000). Nevertheless, the extent to which the shock waves affect macroscopic parameters of the spray, and the atomization of the fuel is currently unknown. The origin of these differences could be related to the depression that is created behind the spray-ambient impact region, the so-called Mach cone (MacPhee et al., 2004). This will be the subject of a proposed future study.

Since these significant differences have been observed, we have analyzed the results from the SF_6 and N_2 separately.

5.2 Spray tip penetration

In the theoretical analysis presented previously, it is assumed that injection rate shape is perfectly rectangular. However, in real cases the needle lift is not instantaneous and, as a consequence, injection rate is not rectangular and its shape changes with the injection conditions. This can be due to two different causes (Payri et al., 2004c) :

- The dynamic behavior of the common-rail system depending on the injection pressure.
- The variation of the orifice's effective section which is a function of needle position and orifice size.

Figure 8 shows the measured injection rate of one of the nozzles (ϕ_o=183 μm) for the three injection pressures together with a theoretical rectangular curve.

The equipment used to measure the injection rate is a standard Injection Rate Discharge Curve Indicator (IRDCI) described in Bosch (1966) and it enables for data describing the chronological sequence of an individual fuel-injection event to be displayed and recorded.

To obtain a good estimation of the experimental errors, several repetitive measurements were carried out at the same test point (energizing time, rail pressure and backpressure) and the obtained dispersion was of about 0.6%, with proper calibration of the equipment.

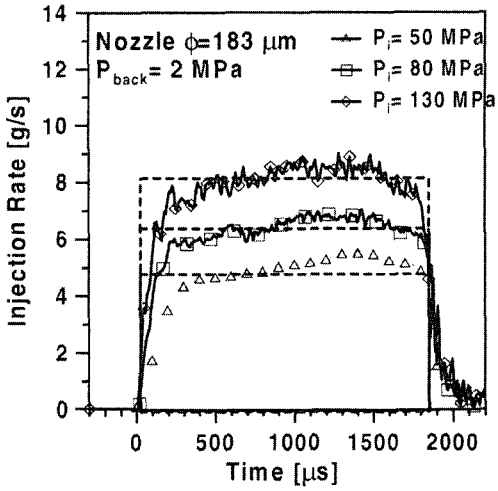

Fig. 8 Measurements of mass injection rate compared with the theoretical rectangular curve. ϕ_o=183 μm

It can be noted (Figure 8) that the increase in the injection pressure for a given nozzle implies steeper slopes during needle rising, and consequently the injection rate shape for higher injection pressures is closer to the rectangular one.

A similar conclusion is reached to if, for a given injection pressure, the injection rates of different nozzles with different diameters are compared : it is observed that the injection rate shape for smaller nozzle holes is closer to the rectangular one, i.e., the plateau of the curve is reached earlier (Arrègle et al., 1999).

As expected, both phenomena influence the spray penetration curve at the start of the injection where the mass flow rate does not have a rectangular shape, and so, the instantaneous momentum flux through the hole is smaller than the theoretical one. In our experiments, this was reflected as a change in the spray tip penetration curves.

In Figures 9 and 10 the spray tip penetration as a function of time is depicted in logarithmic scale for two nozzles (ϕ_o=183 μm, ϕ_o=119 μm), two injection pressures (P_i=50 MPa, P_i=80 MPa),

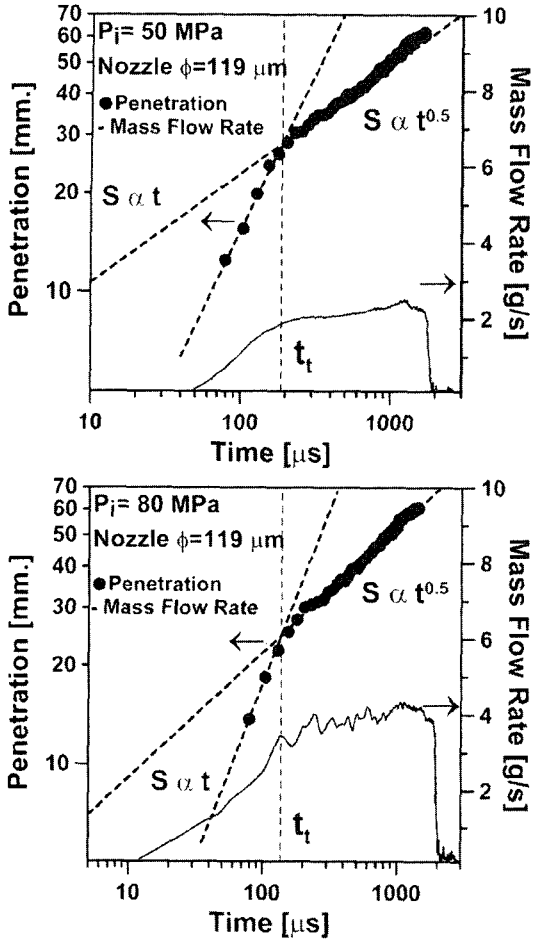

Fig. 9 Mass flow rate and spray tip penetration as a function of time in logarithmic scale for nozzle 119 μm. Identification of transition time, t_t

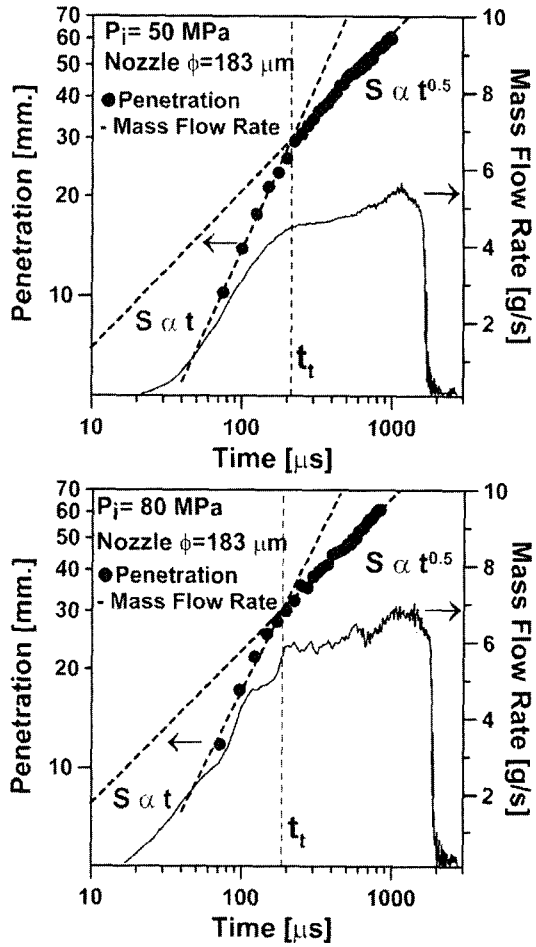

Fig. 10 Mass flow rate and spray tip penetration as a function of time in logarithmic scale for nozzle 183 μm. Identification of transition time, t_t

P_{back}=2 MPa, ρ_a=24 Kg/m^3 in the N_2 test rig. The experimentally-determined penetration (represented in logarithmic scale) can clearly be fitted into two straight lines with different slopes. As can be seen in the both figures, at the beginning of the injection process, the penetration's dependence of time can be expressed as $S \propto t$ (a linear function of time), whilst from an instant, t_t, after the start of injection, the penetration-time relationship is $S \propto t^{0.5}$. This transition time (t_t) has been referenced frequently in previous presented literature (Hiroyasu and Arai, 1990; Naber and Siebers, 1996). Hiroyasu and Arai (1990) were observing a transition time that they called the "break-up time" at which a transition is made from a linear time dependence of the penetration to a square root dependence. According to Hiroyasu and Arai, this time is related to the break-up length. On the other hand, Naber and Siebers (1996) consider this as being the instant when the spray mixture changes from being dominated by injected liquid to being dominated by entrained gas.

In the present experiments, this time (t_t) has been clearly identified with the transient period at which the mass flow rate (and thus the momentum flux) is increasing due to the variation of the nozzle's effective section as a function of needle

opening. For injection times lower than the transition time t_t the penetration is influenced by the increasing mass flow rate. In Figures 9 and 10 is also depicted the mass flow rate as a function of time. It can be observed that the point at which the fitted functions change from one to the other (t_t) coincides with the instant at which the mass flow rate reaches its maximum value. The variations in the maximum value of the mass flow rate in Figure 9 are due to pressure fluctuations in the nozzle, inherent to the injection process (Payri et al., 2004c ; Kim et al, 2003).

The transition time has been determined for all the operating points of Table 2, and in a first step, in order to compare with the theoretical analysis established in the background, the results will focus on the times $t>t_t$, i.e, the stable part of the mass flow rate. The explanation for the linear penetration dependence with time for $t<t_t$ will be the subject of a proposed future study.

As a first step in the analysis of penetration laws, the experimental results have been fitted to the following expression in both SF_6 and N_2 test rig :

$$S(t)=k\cdot\rho_a^a\cdot\Delta P^b\cdot\phi_o^c\cdot t^d \qquad (4)$$

From here, the values for the exponents presented in Table 4 were deduced.

Table 4 Values of the exponents for spray tip penetration correlation

	EXPONENT	FIT	Confidence Int.
Nitrogen test rig	k	0.573	[0.548, 0.597]
	a	−0.336	[−0.337, −0.335]
	b	0.287	[0.286, 0.289]
	c	0.367	[0.364, 0.371]
	d	0.49	[0.489, 0.492]
	R-Squared=97.69%		
	EXPONENT	FIT	Confidence Int.
SF_6 test rig	k	0.235	[0.206, 0.264]
	a	−0.355	[−0.355, −0.346]
	b	0.329	[0.324, 0.333]
	c	0.314	[0.304, 0.325]
	d	0.526	[0.522, 0.529]
	R-Squared=94.61%		

The results demonstrate that all the parameters included in the correlation play an important role. The R-Squared value in both cases suggests high confidence on the correlation results from the statistics point of view. If the results from N_2 and SF_6 test rigs were compared, one could observe a better correlation for the former. The exponents affecting each parameters are different from those provided by the dimensional analysis, with the exponents obtained from results in N_2 being closer to these.

The experimental results appear to be very consistent with previous experimental research in Diesel sprays at high ambient density (Arrègle et al., 1999 ; Naber and Siebers, 1996 ; Payri et al., 1996). For example, the ambient density exponent (−0.34), which differs from the theoretical (−0.25), is almost exactly the same as that found by Naber and Siebers (−0.35) (Naber and Siebers, 1996).

However, it must be noted that the dimensional analysis did not take into account the variations of the spray cone angle between the different sprays, which can be significant as will be commented below.

To account for such variations on the spray cone angle, Wakuri et al.(1966) proposed a spray tip penetration correlation which includes it as an additional variable. To compare with this correlation, the experimental measurements of spray tip penetration have been fitted again, including the spray cone angle too :

$$S(t)=k\cdot\rho_a^a\cdot\Delta P^b\cdot\phi_o^c\cdot t^d\cdot\tan\left(\frac{\theta}{2}\right)^{-0.5} \qquad (5)$$

The results obtained in this case for both test rigs can be found in Table 5.

The R-squared value suggests again good confidence in the correlation obtained, with values slightly higher. Furthermore, the exponents now obtained considering the dependence of penetration with the spray cone angle agree almost perfectly with those obtained from the dimensional analysis, especially for the N_2 results.

Figure 11 shows the comparison of the observed penetration, in the N_2 test rig, compared to those predicted by the previous regression. In

Table 5 Values of the exponents of equation (5) for spray tip penetration

	EXPONENT	FIT	Confidence Int.
Nitrogen test rig	k	0.652	[0.625, 0.678]
	a	−0.268	[−0.269, −0.267]
	b	0.254	[0.253, 0.256]
	c	0.417	[0.413, 0.420]
	d	0.513	[0.511, 0.514]
	e	−0.5	−
	R-Squared=98.14%		
	EXPONENT	FIT	Confidence Int.
SF_6 test rig	k	0.155	[0.136, 0.174]
	a	−0.228	[−0.232, −0.224]
	b	0.336	[0.331, 0.341]
	c	0.416	[0.407, 0.426]
	d	0.549	[0.545, 0.552]
	e	−0.5	−
	R-Squared=94.79%		

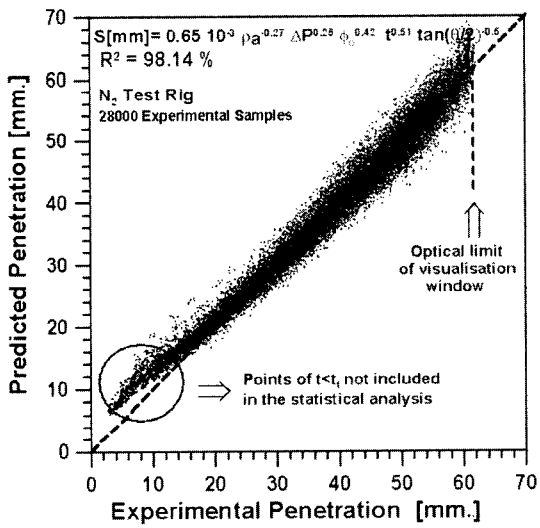

Fig. 11 Experimental penetration versus penetration predicted by eq. (5) and considering exponents of Table 4 (N_2 test rig)

this figure, the points that do not fit very well with the regression and can be seen inside the circle represent the measurements of penetration for $t<t_t$. Although they are represented in the figure, they have not been taken into account for the statistical analysis of results. It has to be

Table 6 Values of k in equation (5) for spray tip penetration

	EXPONENT	FIT	Confidence Int.
N_2 test rig	k	2.839	[2.836, 2.841]
	R-Squared=97.69%		
	EXPONENT	FIT	Confidence Int.
SF_6 test rig	k	2.948	[2.941, 2.954]
	R-Squared=90.6%		

mentioned as well that spray penetrations higher than 60 mm can not be characterized because of the dimensions of the test rig and its windows.

Finally, the experimental results are fitted to the theoretical expression:

$$S(t)=k\cdot\rho_a^{-0.25}\cdot\Delta P^{0.25}\cdot\phi_o^{0.5}\cdot t^{0.5} \qquad (6)$$

where the value of the constant k, and the degree of correlation obtained are presented in Table 6.

The R-square value obtained suggest good confidence in the correlation obtained specially for the N_2 results which is in agreement with the theoretical dimensional analysis performed (equation 3).

6. Conclusions

The influence of the main injection parameters on the spray tip penetration of Diesel Sprays generated by a common rail injection system has been characterized and quantified. This characterization has been performed in two different injection test rigs that can reproduce the real engine in-cylinder air density and pressure. The results obtained have been used to confirm various correlations available in the literature and to extend them to current Diesel injection conditions with small nozzle hole diameters and high injection pressure values. From this work some important conclusions can be drawn:

(1) Given a certain chamber density, there have been observed differences between the two test rigs, regarding the spray tip penetration and the spray cone angle. Penetration in the SF_6 case is on average around 6% higher than in N_2 case and the spray cone angle measured in the former

can be about 10% smaller than in latter. Cavitation phenomena as well as small differences in the pressure drop were discarded as possible causes. The generation of shock waves in SF_6 and their absence in N_2 is one possible cause that must be studied in the future.

(2) The injection rate shape affects spray tip penetration : while at the beginning of the injection process the penetration is a linear function of time, from the instant t_t after the start of injection, the penetration is a function of the squared root of the time. This transition time (t_t) has been clearly identified as the transient period after the start of injection at which the mass flow rate is increasing due to the variation of the nozzle's effective section as a function of needle opening.

(3) The influence on penetration of each test parameter (gas density, diameter, time and pressure drop), has been clearly evidenced in this work. Results demonstrate that all the parameters included in the correlation play an important role.

(4) The correlations obtained from this work predict the spray tip penetration with a high degree of accuracy even if the angle is not included as a factor (equation 4). A simple dimensional analysis has led to the same expression (equation 3). A better level of confidence is obtained if spray cone angle is taken into consideration.

(5) If results from both test rigs are compared, it can be concluded that the correlations obtained from the N_2 test rig show higher confidence in predicting penetration than those from the SF_6 test rig, and are closer to the values expected theoretically.

Acknowledgments

The authors would like to thank Jose Enrique del Rey (From CMT-Motores Tĕrmicos. Universidad Politécnica de Valencia) for his collaboration in the experimental measurements.

References

Arai, M., Shimizu, M. and Hiroyasu, H., 1991, "Similarity between the Break-up Lengths of a High Speed Liquid Jet in Atmospheric and Pressurized Conditions," In ICLASS-91, Gaithersburg, Maryland.

Arrégle, J., Pastor, J. V. and Ruiz, S., 1999, "The Influence of Injection Parameters on Diesel Spray Characteristics," SAE Paper 1999-01-0200.

Bosch, W., 1966, "The Fuel Rate Indicator : A New Measuring Instrument for Display of the Characteristics of Individual Injection," SAE Paper 660749.

Cheong, S. -K., Liu, J., Shu, D., Wang, J. and Powell, C. F., 2004, "Effects of Ambient Pressure on Dynamics of Near- Nozzle Diesel Sprays Studied by Ultrafast X-Radiography," SAE Paper 2004-01-2026.

Dent, J. C., 1971, "A Basis for the Comparison of Various Experimental Methods for Studying Spray Penetration," SAE Paper 710571.

Desantes, J. M., Payri, R, Salvador, F. J. abd Gimeno, J., 2003, "Measurements of Spray Momentum for the Study of Cavitation in Diesel Injection Nozzles," SAE Paper 2003-01-0703.

Desantes, J. M., Payri, R., Pastor, J. M. and Gimeno, J., 2005, "Experimental Analysis of Fuel Evaporation in Diesel Sprays. Part I. Nozzle characterization," *Atomization and Sprays*, Vol. 15, pp. 489~516.

Hay, N. and Jones, P. L., 1972, "Comparison of the Various Correlations for Spray Penetration," SAE Paper 720776.

Hiroyasu, H. and Arai, M., 1990, "Structures of Fuel Sprays in Diesel Engines," SAE Paper 900475.

Hurly, J. J., Defibaugh, D. R. and Moldover, M. R., 2000, "Thermodynamic Properties of SF_6," *Int. J. Thermophysics* 2000, 21, pp. 739~765.

Kim, C. H. and Lee, J. S., 2003, "An Analytical Study on the Performance Analysis of a Unit-Injector System of a Diesel Engine," *KSME International Journal*, Vol. 17, No. 1, pp. 146~156.

Koo, J. Y., 2003, "The Effects of Injector Nozzle Geometry and Operating Pressure Conditions on the Transient Fuel Spray Behavior," *KSME International Journal*, Vol. 17, No. 3, pp. 617~625.

Macian, V., Payri, R., Margot, X. and Salvador,

F. J., 2003a, "A CFD Analysis of the Influence of Diesel Nozzle Geometry on the inception of Cavitation," *Atom Sprays* 2003, 13, pp. 579~604.

Macian, V., Bermúdez, V., Payri, R. and Gimeno, J., 2003b, "New Technique for the Determination of the Internal Geometry of Diesel Nozzle with the use of the Silicone Methodology," *Exp. Tech* 2003, 27(2), pp. 39~43.

MacPhee, A. G., Tate, M. W., Powell, C. F., Yue, Y., Renzi, M. J. et al., 2002, "X-ray Imaging of Shock Waves Generated by High-pressure Fuel Sprays," *Science*, Vol. 295, pp. 1261~1263.

Naber, J. and Siebers, D.L., 1996, "Effects of gas density and vaporisation on penetration and dispersion of Diesel sprays," SAE Paper 960034.

Pastor, J. V, Payri, R., López, J. J. and Juliá, J. E., 2003, "Effect of Injector Nozzle Geometry of Diesel Engines on the Macroscopic Spray Characteristics by Means of Optical Techniques," Fuel Injection Systems. ImechE Conference Transactions. C610/014/2003, pp. 73~82.

Pastor, J. V., Arrègle, J. and Palomares, A., 2001, "Diesel Spray Image Segmentation with a Likelihood Ratio Test," Applied Optics, Vol. 40, No. 17, pp. 2876~2885.

Payri, F., Desantes, J. M. and Arrègle, J., 1996, "Characterization of D.I. Diesel Sprays in High Density Conditions," SAE Paper 960774.

Payri, F., Bermúdez, V., Payri, R. and Salvador, F. J., 2004, "The Influence of Cavitation on the Internal Flow and the Spray Characteristics in Diesel Injection Nozzles," Fuel 2004, 83, 419-31.

Payri, R., Margot, X. and Salvador, F. J., 2002, "A Numerical Study of the Influence of Diesel Nozzle Geometry on the Inner Cavitating Flow," SAE Paper 2002-01-215.

Payri, R., Molina, S., Salvador, F. J. and Gimeno, J., 2004a, "A Study of the Relation between Nozzle Geometry, Internal Flow and Sprays Characteristics in Diesel Fuel Injection Systems," *KSME International Journal*, Vol. 18, No. 7, pp. 1222~1235.

Payri, R., Guardiola, C., Salvador, F. J. and Gimeno, J., 2004b, "Critical Cavitation Number Determination in Diesel Injection Nozzles," *Experimental Techniques*, Vol. 28, No. 3, pp. 49~51.

Payri, R., Climent, H., Salvador, F.J., Favennec, A. G., 2004c, "Diesel Injection System Modelling. Methodology and Application for a First-generation Common Rail System," *Proc. Instn. Mech. Engrs.*, Vol. 218, Part D : Automobile Engineering, pp. 81~91.

Payri, R., García, J.M., Salvador, F.J., Gimeno, J., 2005, "Using Spray Momentum Flux Measurements to Understand the Influence of Diesel Nozzle Geometry on Spray Characteristics," Fuel 2005, 84, pp. 551~561.

Wakuri, Y., Fujii, M., Amitani, T. and Tsuneya, R., 1960, "Studies of the Penetration of a Fuel Spray in a Diesel Engine," *Bull. J.S.M.E.*, 3(9), pp. 123~130.